Electronic Supplementary Information

Tunable Nonlinear Optical Responses and Carrier Dynamics of Two-Dimensional Antimonene Nanosheets

Lei Zhang,[a] Shah Fahad,[b] Hao-Ran Wu,[a] Tao-Tao Dong,[a] Zi-Zhen Chen,[a] Ze-Qi Zhang,[a] Rui-Tong Liu,[a] Xin-Ping Zhai,[a] Xiang-Yang Li,[a] Xian Fei,[a] Qi-Wei Song,[a] Zhe-Ji Wang,[a] Li-Chuan Chen, [a] Chun-Lin Sun,[a] Yong Peng,[b] Qiang Wang, [a,*] Hao-Li Zhang [a,c *]

a State Key Laboratory of Applied Organic Chemistry (SKLAOC), Key Laboratory of Special Function Materials and Structure Design (MOE), College of Chemistry and Chemical Engineering, Lanzhou University, Lanzhou, 730000, P. R. China

b Key Laboratory of Magnetism and Magnetic Materials of Ministry of Education, School of Physical Science and Technology, Lanzhou University, Lanzhou, 730000, P. R. China

c Tianjin Key Laboratory of Molecular Optoelectronic Sciences, Department of Chemistry, Tianjin University, Collaborative Innovation Center of Chemical Science and Engineering (Tianjin), Tianjin University, Tianjin 300072, P. R. China

E-mail: qiangwang@lzu.edu.cn;
haoli.zhang@lzu.edu.cn

Experimental section

Materials

The Sb shots were purchased from Aladdin. N-Hexane was from Tianjin Rionlon Bohua Pharmaceutical Chemical Company Limited and was distilled and refluxed over a sodium wire under argon atmosphere before use. N-BuLi (2.5 M) in hexane was purchased from Beijing Ino-Chem Technology Company Limited. Ethanol absolute was from Sinopharm Chemical Reagent Company Limited. Deionized water (resistivity: 18.3 MΩ•cm) was used throughout the experiment. Sb_2O_3 was purchased from Aladdin.

Synthetic procedures

Sb shots were grounded into powders using an agate mortar first. To prepare Sb nanosheets, Sb powder (122 mg, 1 mmol) was added in a round-bottom two-necked flask equipped with an Allihn condenser. Under an argon atmosphere, 2.5 mL of n-BuLi (2.5 M) in hexane was added. Then dry n-hexane (20 mL) was added. The dispersion was heated to 85 ℃ for 48 hours. After reflux, the brownish solution was quenched by the addition of 7.5 mL ethanol absolute. The solution was washed with ethanol and DI water three times respectively. After the remove of side-products, the sample was redispersed in ethanol under the sonication for 60 min. The sample was centrifuged at 1000 rpm for 10 min to remove unexfoliated bulk and the top two-thirds were collected.

Characterization

Centrifugation was performed on the XiangYi TG16-W centrifuge. The relative centrifugal force (RCF) under different rotation speeds is collected in **Table S1**. UV-vis-NIR absorption spectra were collected on a TU-1810 Spectrophotometer (Beijing Purkinje General Instrument, China). FT-IR spectra were recorded on a Bruker Vertex 70v vacuum spectrometer. The Raman spectra were obtained on a Renishaw Raman Microscope System equipped with an excitation wavelength of 633 nm. XPS measurements were obtained on a PHI-5702 apparatus (Physical Electronics, USA), which has a monochromated AlKa source. The TEM micrographs were acquired

using Talos F200C (FEI, USA) at operating voltages of 200 kV. The height and amplitude features of the products were investigated on an Atomic Force Microscope (AFM) of Agilent 5500. The laser photolysis experiments were performed on an LP920 (Edinburgh Instrument) transient absorption spectrometer. Before the measurements, the samples were purged with nitrogen to remove oxygen (~10 min) in the solution. The Z-scan setup which was equipped with a Q-switched Nd:YAG laser (Continuum, Model Surelite SL-I-10) was performed to measure the nonlinear optical responses of the as-prepared samples.

SEM Characterization of Sb bulk

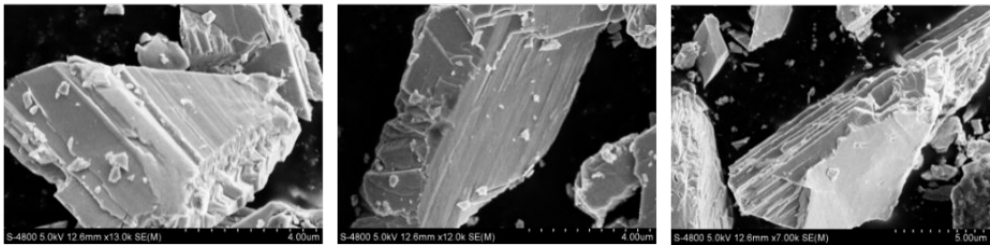

Figure S1. The typical SEM images of Sb bulk.

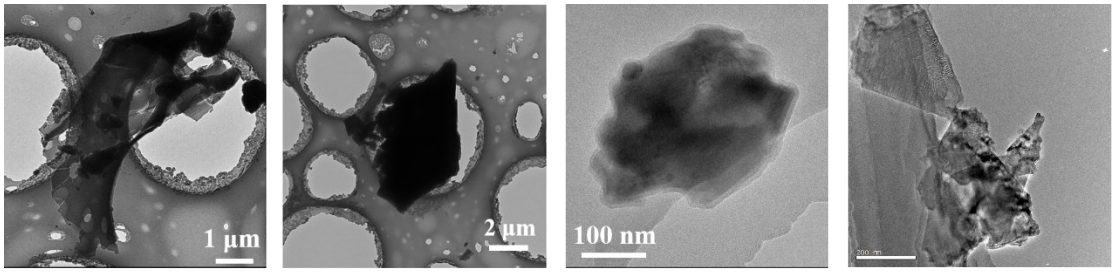

Figure S2. The typical TEM images of Sb nanosheets.

A stair-like layered morphology can be observed indicating the potential to be exfoliated into 2D nanosheets. After intercalation, a large flat plain can be observed in TEM characterization.

Chemical component analysis of Sb bulk, Sb nanosheets and Sb oxides

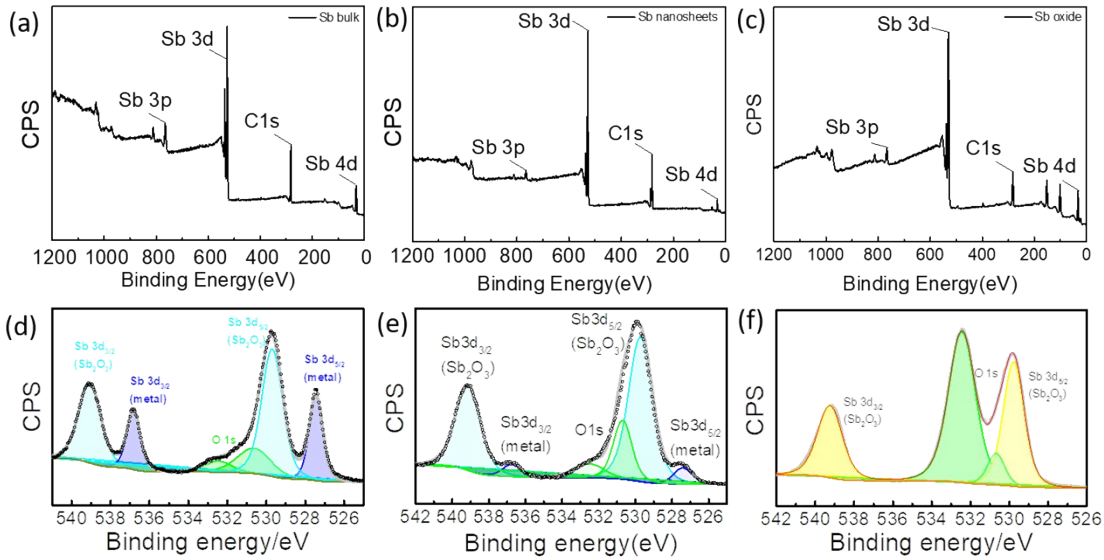

Figure S3. (a-c) XPS spectra for Sb bulk, Sb nanosheets and Sb oxide. (d-e) representing the corresponding survey spectra of Sb bulk, Sb nanosheets and Sb oxide, respectively.

Sb bulk and Sb nanosheets both exhibit the signals of Sb and Sb oxide. After intercalation and washing, the Sb component decreases while the Sb-O increases. We can speculate that the increasing of the oxide component is due to the involvement of the washing step with water. Because Sb nanosheets were totally oxidized into Sb_2O_3 [1]after the redispersion in water for 2 months, which is shown in (c) and (f).

To estimate the inelastic mean free path (IMFP), λ, the following formula which was developed by Seah and Dench is applied:[2]

$$IMFP = \lambda = 2170KE^{-2} + 0.72(aKE)^{0.5}$$

Where λ is in units of monolayers, a represents the thickness of monolayer (nm), KE stands for the electron kinetic energy (in eV).[3] The monolayer thickness (a) is calculated in the following formula:

$$a = \sqrt[3]{\frac{M_W}{\rho \cdot n \cdot N}}$$

Where M_w is the molecular weight, ρ represents the volume density, n stands for the atom numbers and N is the Avogadro's number.

The calculated IMFP is 11.77 monolayers and the estimated thickness of the surface oxides is about 3.03 nm.

Stability study of Sb solubility in ethanol

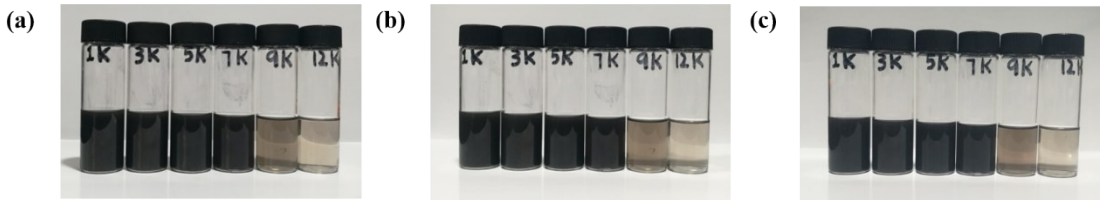

Figure S4. The images of Sb nanosheets dispersion prepared through gradient centrifugation for (a) 0 day, (b) 4 days and (c) 8 days (solvent: ethanol).

Yield Calculation of the intercalation method

Table S1. Yield calculation of intercalating Sb

Relative centrifugal force (RCF)	630g	1700g	3400g	5600g	10000g
centrifugation speed	3k	5k	7k	9k	12k
m (mg)	9.78	5.68	3.89	3.93	6.47
Yield	8.02%	4.66%	3.19%	3.22%	5.30%
Total yield			24.39%		

Table S2. Yield comparison of top-down methods to produce Sb nanosheets

Starting mass	Method	Yield	Reference[a]
10 mg	Wet-ball milling + tip sonication	37%	4
80 mg	Bath sonication	~5%	5
10 mg	Bath sonication	<1%	6
500 mg	Pregrinding + tip sonication	40.73%	7
100 mg	Bath sonication	1%	8
122 mg	Li^+ intercalation + bath sonication[b]	24.39%	This work
122 mg	Bath sonication[c]	5.89%	This work
244 mg	Li^+ intercalation + bath sonication[d]	19.64%	This work
1220 mg	Li^+ intercalation + bath sonication[d]	15.20%	This work

[a] Literatures are listed in **Reference**.[4-8]

[b] Conditions: 1 mmol (~122 mg) Sb powder was dispersed into 2.5 mL *n*-BuLi and 10 mL n-hexane. The mixture was reflux for 48 hours. After washing steps, the sample was vacuum dried and re-dispersed into ethanol through sonication for 1h. Gradient centrifugation was carried out to produce different size-ranged Sb nanosheets. Then the products were vacuum dried overnight and weighted to calculate the yield.

[c] Control experiment conditions: Control experiment was carried out as below: 122 mg Sb powder was added in 12.5 mL mixed solvent (iso-propanol : water = 4:1) without any pre-processing treatment. The mixture was sonicated for 48 hours and centrifuged at 1000 rpm for 10 min to remove unexfoliated bulk and the top two-thirds were collected. Then the dispersion was centrifuged at 12000 rpm for 10 min. The collected sediment was dried at 70 ℃ overnight.

[d] Mass-up preparation conditions: Mass-up experiments were prepared through the detailed description in **b** conditions and synthetic procedures. Note *n*-BuLi were added proportionally (sample 1: 2.5 mL *n*-BuLi; sample 2: 5 mL *n*-BuLi; sample 3: 25 mL *n*-BuLi). The reaction time were 48 hours for all the three reactions.

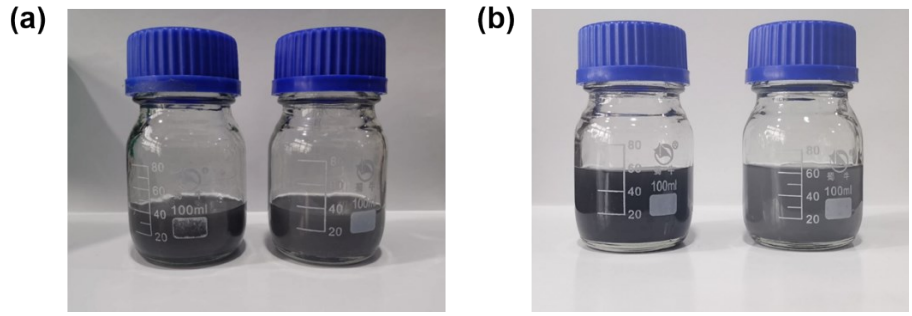

Figure S5. Digital photographs of Sb nanosheets prepared through lithium ion intercalation (left) and liquid phase exfoliation (right). (a) Before 1000 rpm centrifugation for 10 min to remove unexfoliated materials. (b) After the removal of unexfoliated bulk materials.

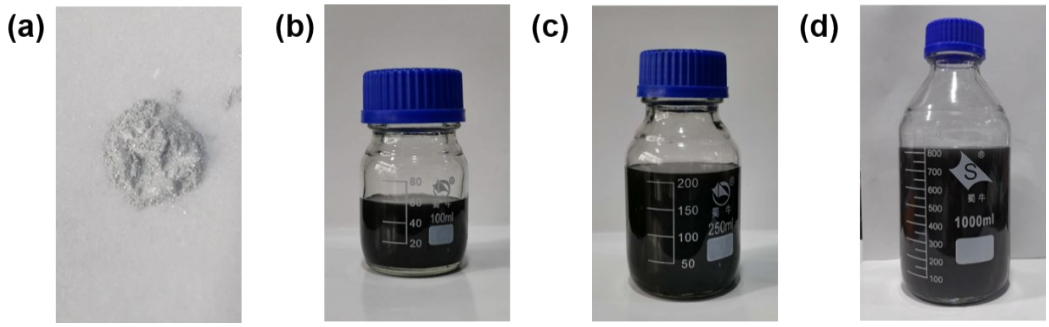

Figure S6. Digital photographs of (a) Sb powder and Sb nanosheets ethanol dispersion prepared through different starting mass of Sb powder: (b) 122 mg (1 mmol); (c) 244 mg (2 mmol); (d) 1220 mg (10 mmol).

Solvent exfoliation is mainly based on weakening the Van der Waals force between layers by sonication in appropriate solvents.[9, 10] The fact that bulk Sb is more difficult to be exfoliated into nanosheets than other layered materials can be attributed to the relative shorter layer distance (0.216 nm) and stronger interlayer interaction. Furthermore, to achieve massive fabrication with high efficiency, the selection of appropriate exfoliating solvent is crucial. There are very few systematic studies on the ideal exfoliation solvents of Sb nanosheets.[4] A rational analysis to both exfoliation efficiency and the solvent effect is essential for the mass production of Sb nanosheets. Besides, ion intercalation is another important top-down method to prepare 2D materials, which uses proper ions, typically alkali and ammonium cation, to intercalate into the interlayer spacing of layered crystals and then exfoliate the bulk. **Figure S5** compared the liquid phase exfoliation and intercalation, and much higher concentration of Sb nanosheets can be observed in intercalation prepared sample. Based on this efficient preparation method, scaleup Sb nanomaterials can be produced even up to gram scale (**Figure S6**).

Spectroscopic characterization of size-ranged Sb nanosheets

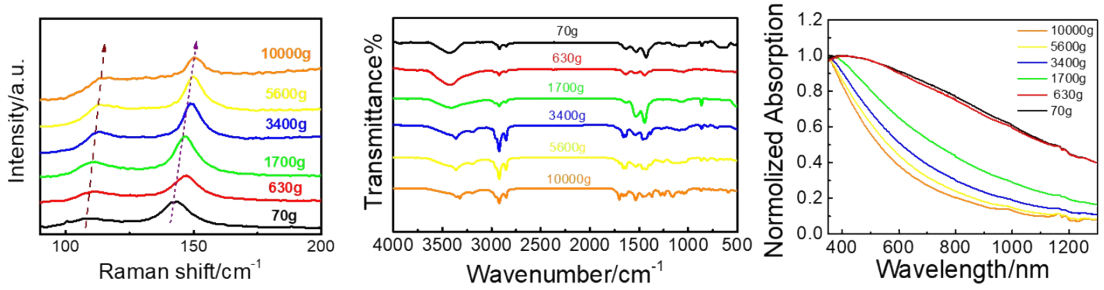

Figure S7. (a) Raman spectra, (b) Infrared spectra and (c) UV-vis-NIR absorption spectra of 70 g c, 1700 g (5k), 3400 g (7k), 5600 g (9k), and 10000 g (12k) rotation force (speed) prepared Sb nanosheets, respectively.

These two peaks in Raman spectra, assigning to the interlayer (E_g, ~110 cm^{-1}) and intralayer (A_{1g}, 140 cm^{-1}) vibration modes of Sb, exhibit a red shift (high Raman shift direction) with the increasing of centrifuging speed. This phenomenon is commonly observed in Van der Waals 2D materials such as black phosphorus and is widely understood as the successful exfoliation of bulk materials into ultrathin 2D nanosheets. Additionally, serval weak peaks located in the region of 700~500 cm^{-1} appears, which can be related to the stretching vibrations of Sb–O.[11] The bands at approximately ~3350 cm^{-1} were assigned to the stretching vibrations of O-H. The signals near to 1739 and 1633 cm^{-1} were ascribed to the deformation of water molecules, indicating the presence of physiosorbed water on the Sb surface.[12] Then the UV-vis-NIR absorption spectra were carried out to investigate the absorption band difference of size-ranged Sb. The absorption intensity deceases with the rotation speed increasing.

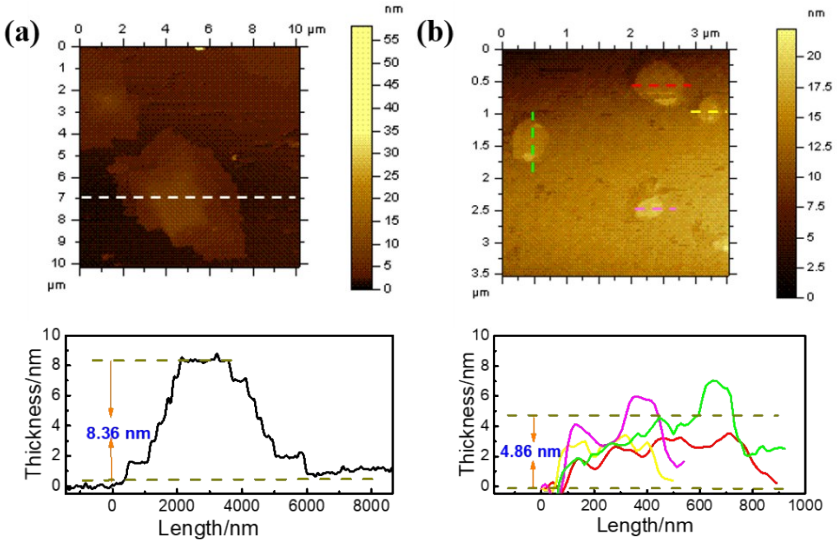

Figure S8. Representative AFM images of (a) 70 g(1k) and (b) 630 g (3k) samples, respectively. The lateral height of each sample is exhibited under the corresponding AFM images.

Microscopic Characterization of size-ranged Sb nanosheets

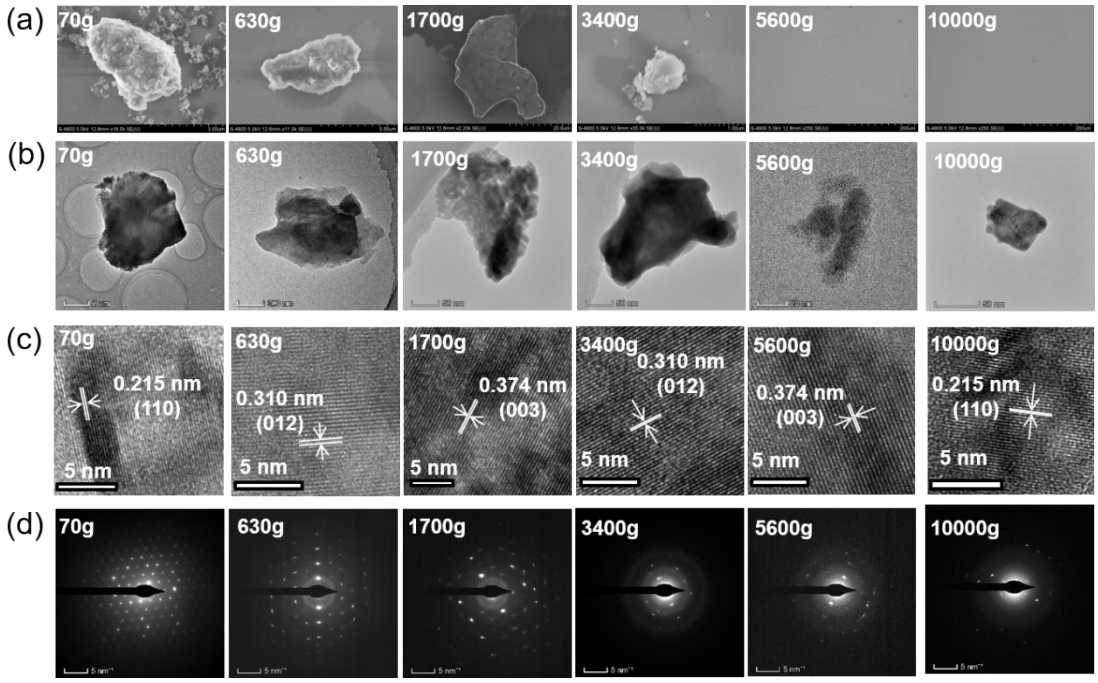

Figure S9. (a) SEM images, (b) TEM images, (c) HR-TEM images and (d) SAED pattern images of 70 g (1k), 630 g (3k), 1700 g (5k), 3400 g (7k), 5600 g (9k), and 10000 g (12k) Sb nanosheets, respectively. Flat sheet structure belongs to typical 2D materials can be observed in SEM and TEM.

The sheet size decreases with the increasing of the rotation speed. Moreover, the lattice fringes assigning to Sb crystal can be extracted in all of the samples. Uniform diffraction spots in the SAED pattern reflects the high quantity in single crystal form.

Solubility and stability study of Sb nanosheets

Since we have obtained Sb nanosheets successfully through the intercalation procedure, it is possible to investigate the solubility of Sb nanosheets in different solvents. The well-known basic principle of solubility is "like dissolves like". However, in many cases, this qualitatively empirical rule cannot work well, especially for polymers and nanomaterials. In order to extract quantitative information, a series of parameters to evaluate solubility was involved to form a semi-empirical correlation, which is the theory of Hansen solubility parameters (HSP). The HSP is defined as the square root of the cohesive energy density:

$$\delta^2 = \delta_D^2 + \delta_P^2 + \delta_H^2$$

$$\delta = \sqrt{CED} = \sqrt{\frac{\Delta H - RT}{V_m}}$$

Where δ_D, δ_P and δ_H are atomic dispersion forces, molecular permanent dipole–permanent dipole forces, and molecular hydrogen bonding. δ is the square root of cohesion energy density (CED). Solvent and solute with similar HSP have a high affinity for each other, which can be evaluated through HSP distance R_a:

$$R_a^2 = 4(\delta_{D,solv} - \delta_{D,solu})^2 + (\delta_{P,solv} - \delta_{P,solu})^2 + (\delta_{H,solv} - \delta_{H,solu})^2$$

R_a, between solute and solvent-based on their respective partial solubility parameter components, can be used as a guide for finding a single efficient solvent for its dispersion. The smaller the Ra value, the better the solubility. It is possible to estimate the HSP of nanomaterials by searching the smallest R_a value. Meanwhile, when we know the HSP of a nanomaterial, it is possible to develop low-cost and low toxic solvent mixture for efficient exfoliation than single-component solvent. The better the solubility, the higher the concentration.

Table S3. HSP parameters of 10 organic solvents[13]

	n-Pentanol	Ether	n-Hexane	Ethanol	Acetone	Acetonitrile	DMF	DCM	NMP	IPA
δ_D	15.9	14.5	14.9	15.8	15.5	15.5	17.4	18.2	18	15.8
δ_P	4.5	2.9	0	8.8	10.4	10.4	13.7	6.3	12.3	6.1
δ_H	13.9	5.1	0	19.4	7	7	11.3	6.1	7.2	16.4

δ	21.6	15.8	14.9	26.6	20	20	24.8	20.3	22.9	23.5

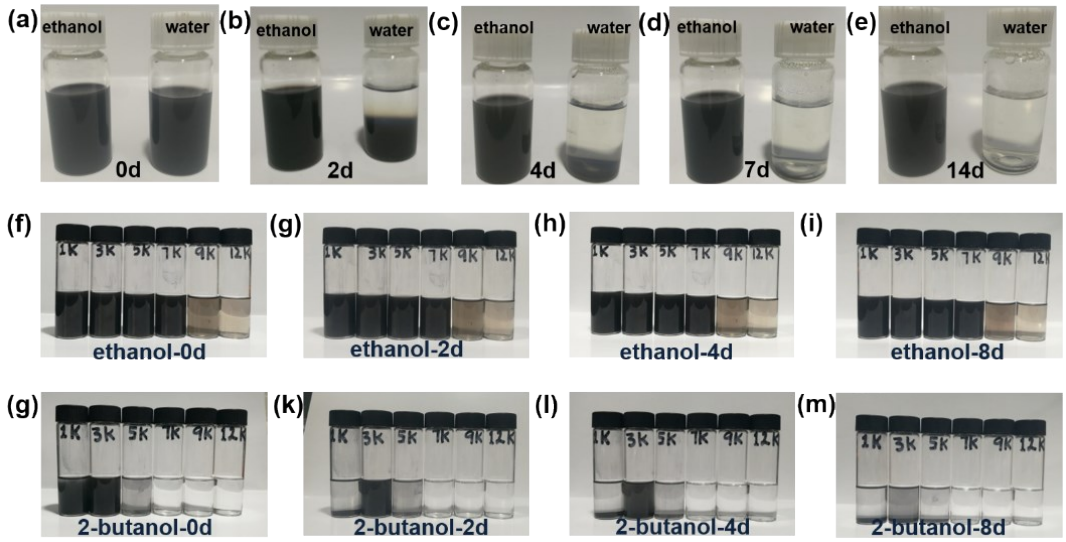

Figure S10. The stability study of the as-prepared Sb nanosheets in ethanol, DI water, and 2-butanol. (a-e) Photographs of Sb nanosheets dispersed in ethanol (left) and DI water (right) for 1 day, 4 days, 7 days and 14 days, respectively. (f-m) Photographs of gradient centrifugated Sb nanosheets (left to right: 70g (1k), 630g (3k), 1700g (5k), 3400g (7k), 5600g (9k) and 10000g (12k), respectively) in ethanol and 2-butanol for 2 days, 4 days and 8 days, respectively.

We tested the solubility of Sb nanosheets in ten different organic solvents and continuously tracked the solution for 20 days. The better the solubility, the higher the concentration. As exhibited in **Figure 3**, ethanol displayed the best solubility to Sb nanosheets as they have the closet HSP parameters. Moreover, after the selection of solvent, a gradient centrifugation procedure was applied to study the solubility of different size-ranged Sb nanosheets. As shown in **Figure S10**, ethanol and 2-butanol were selected to display the size influence of solubility. The concentration of lithium ion intercalated Sb nanosheets mainly distributed among the speed of 1k-7k in ethanol. No deposition was detected even after 8 days, indicating Sb nanosheets with different sizes exhibit excellent solubility and stability in ethanol for a long period. For contrast, the 3k centrifuged Sb nanosheets show the best stability and solubility in 2-butanol, and other centrifuged samples deposited quickly after 2 days. Comparing the HSP parameter of ethanol (δ=26.5) and 2-butanol (δ=22.7), we speculated that 3k centrifuged sample may have a smaller HSP parameter than that of others, endowing it with a better solubility in 2-butanol. In conclusion, ethanol exhibits a good solubility to all size-ranged Sb nanosheets while 2-butanol prefers 3k centrifugated Sb

nanosheets rather than other size products. This also informed us the solubility of one nanomaterial is related to their size as well even though they consist of the same chemical component. In terms of practical applications, ethanol displays a much facile process in concentration or removement to meet diverse industrial requirements.

Meanwhile, the stability of Sb in DI water was also tested. As we know, the HSP of ethanol (δ=26.5, δ_D=16.2, δ_P=10.8, δ_H=16.8) is larger than that of DI water (δ=47.8, δ_D=15.6, δ_P=16, δ_H=42.3), especially in the hydrogen bond part.

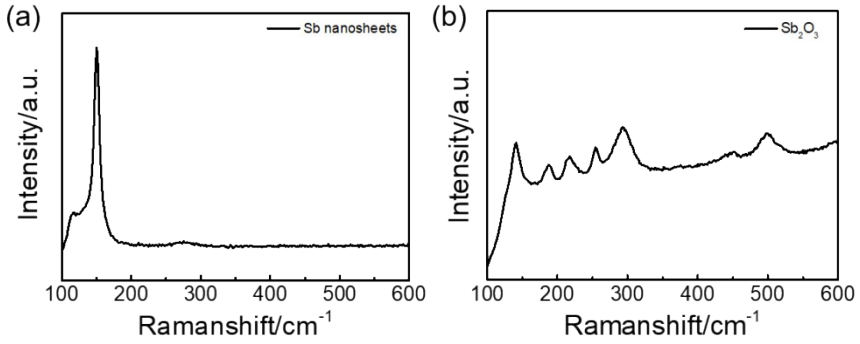

Figure S11. Raman spectra of (a) Sb nanosheets and (b) white deposition.

It is predictable that DI water cannot dissolve Sb nanosheets well. Indeed, we did observe the quick deposition of Sb nanosheets in DI water quickly in 1 day. However, we found for the first time the instability of Sb nanosheets in DI water. As shown in **Figure S11**, the deposition turned to grey in 6 days and totally white in 14 days. We tested the Raman signals of the samples dissolved in ethanol and water. The results are quite different. The two-peak signals of ethanol displayed a similar Raman response to the bulk Sb while these peaks can no long be detected in the water dispersion. Serval new peaks instead of the Sb metal signals were demonstrated in **Figure S11b**. These new peaks located at 141, 189, 217, 254, 292, and 498 cm^{-1} are in well agree with the characteristic peaks of Sb_2O_3. Raman spectra proved that the white can be assigned to antimony oxide. This indicates that Sb nanosheets can be oxidized in plenty of DI water.

NLO property study

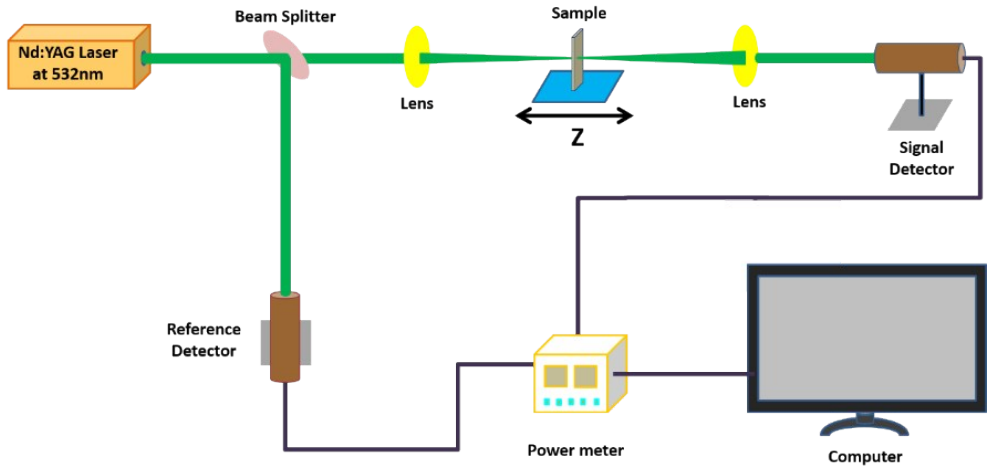

Scheme S1. Experimental setup of Z-scan measurements. The 4 ns (FWHM), 532 nm laser pulses with a repetition rate of 10 Hz from a frequency-double Q-switched Nd:YAG laser was used as the light source. The output laser beam exhibiting a nearly Gaussian distribution was split into two beams: a reference beam and a signal beam. The former beam is to monitor energy fluctuations while the later beam in a tightly focused geometry is passing through the sample. The Sb dispersion was contained in a quartz cell, which was placed on a translation stage controlled by a computer that moved along the z-axis with respect to the focal point of a 410 mm convex lens.

Two corresponding pyroelectric detectors were used to record the changes in two laser beams. Under the open aperture Z-scan mode, the aperture located before the signal beam detector was kept open and measured the intensity change during the movement of Sb dispersion through the z axis. The reference laser beam was simultaneously recorded by another pyroelectric detector. In order to obtain the nonlinear absorption curve, both of the intensities were collected from reference and signal detectors, respectively.

The obtained Z-scan curve is the normalized transmittance (T_{norm}) as a function of the sample position. Herein, we used T_{norm}, which equals to the ratio of nonlinear and linear transmittance. Three typical results can be obtained through the Z-scan technique: (1) The value of T_{norm} maintaining 1.0 indicates no NLO behavior is observed in the material. (2) When the value of T_{norm} is above 1.0, saturable absorption (SA) is observed. (3) In contrast, the value of T_{norm} is below 1.0 indicates reverse saturable absorption (RSA) behavior in the sample.

The Z-scan data were fitted to the nonlinear transmission equation using a sum of

two nonlinear absorptions with opposite signs:

$$\alpha\ (I)\ = \frac{\alpha_0}{1+\left(\frac{I}{I_s}\right)} + \beta I$$

where α_0, I, I_s, and β are the linear absorption coefficient, incident laser intensity, saturable intensity, and effective nonlinear coefficient, respectively. The term $\alpha_0/(1+I/I_s)$ represents the SA part, which increases when I_s arises; whereas a higher β will increase the contribution of RSA. Based on this equation, the Z-scan curves were fitted to evaluate the value of I_s and β, respectively. The corresponding results were exhibited in **Table 1** in detail.

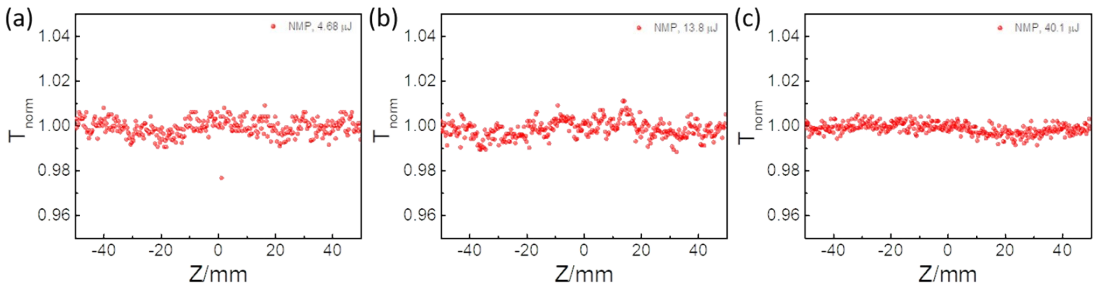

Figure S12. Z-scan results of NMP under (a) 4.68 μJ, (b) 13.8 μJ and 40.1 μJ.

No NLO response was observed in NMP, indicating the SA or RSA signal originates from 2D nanosheets instead of solvent.

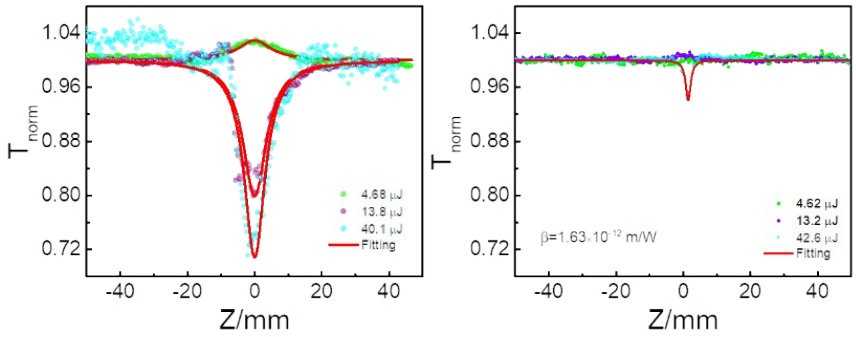

Figure S13. Z-scan open aperture and fitted curves (solid curves) for the samples of the 10000 g Sb nanosheets (left) dispersion and Sb_2O_3 dispersion (right) (solvent: NMP). The linear transmittance of both samples was adjusted to ~0.70 in NMP at the excitation of 532 nm.

Transient absorption spectra (TAS) study on size-ranged Sb nanosheets

The pump-probe technique is utilized in the transient absorption spectroscopy. Briefly, the sample is excited from its ground states by a pump light, and a probe light is interrogated the sample at right angles to the path of the pump pulse. The time delay between the pump and probe light usually varies from femtosecond to microsecond time scale. The transmission property of probe light is collected to compare the transmittance changes before, during and after the exciting pulse. The changes of transmission reflect different molecular excited state dynamics such as excited-state absorption, ground-state bleaching and stimulated emission.[14]

1. **Laser photolysis measurement for nanosecond timescale TAS study**

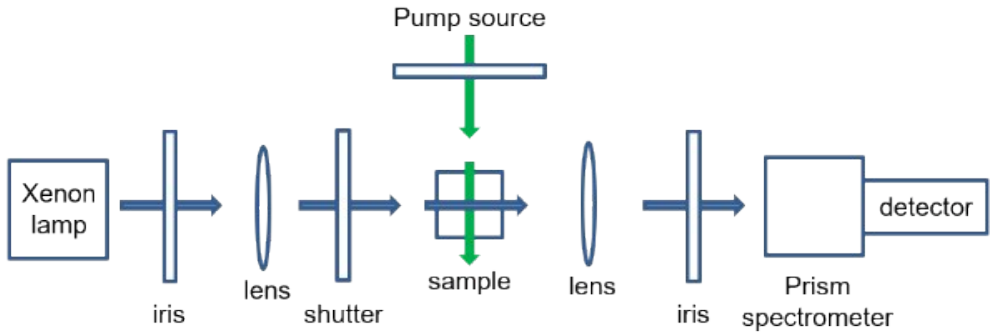

Scheme S2. representation of a laser flash spectrometer setup. The sample is excited by the pump pulse source, while xenon lamp is employed as the probe light to pass through the sample at right angles to the path of the pump pulse. After passing through the sample, the transmitted probe light is then collected to a prism spectrometer or by a CCD camera.

In this work, laser photolysis experiments were performed on an LP920 (Edinburgh Instrument) transient absorption spectrometer equipped with kinetic (PMT) and spectral (ICCD) dual detection modes. The pump laser was set as 532 nm to excite gradient centrifugated Sb nanosheets dispersed in NMP. The detailed experimental setup is shown in **Scheme S2**. The decay curves probed at 550 nm is exhibited in **Figure S14**.

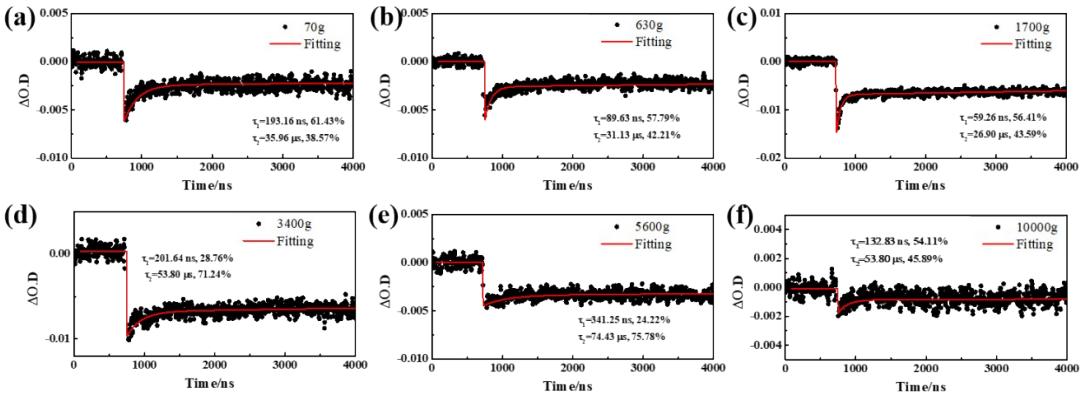

Figure S14. (a-f) Decay curves probed at 550 nm (pump excitation wavelength was 532 nm) of the Sb nanosheets prepared through different centrifugated speed. Centrifuging speeds are 1k, 3k, 5k, 7k, 9k and 12k, respectively. All samples are dissolved in NMP before the test.

Two lifetime components can be extracted including a short one on the ns timescale and a long one on the μs timescale in all of the six samples. We attribute the two long components to the trap-related processes, which have been also observed in other 2D materials.[15]

2. TAS study of Sb nanosheets on the femtosecond timescale

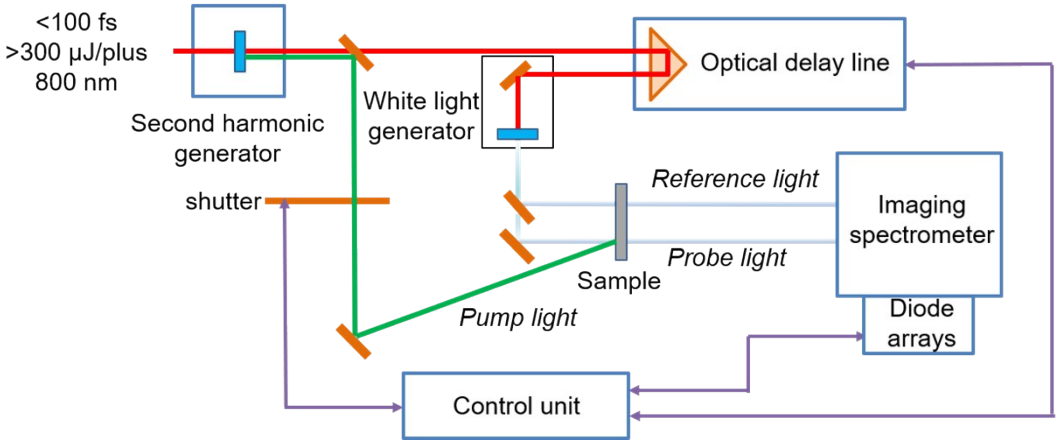

Scheme S3. Schematic representation of femtosecond transient absorption spectroscopy.

Scheme S3 illustrates the setup of femtosecond transient absorption spectroscopy (fs-TAS), in which the laser source was a Coherent Legend Elite regenerative amplifier (<100 fs, 1 KHz, 800 nm) that was seeded by a Coherent Chameleon oscillator (75 fs, 80 MHz). 400 nm wavelength pump laser pulses were generated from a Light Conversion OPerA-Solo optical parametric amplifier (285-2600 nm). The available broadband probe wavelength was from the UV to the NIR range (350–1600 nm). Sb nanosheets dispersion was stored in a quartz cuvette during the TAS

measurement. All of the measurements were performed at room temperature unless otherwise specified. The collected data were analyzed using Surface Xplore software (Ultrafast Systems, LLC).

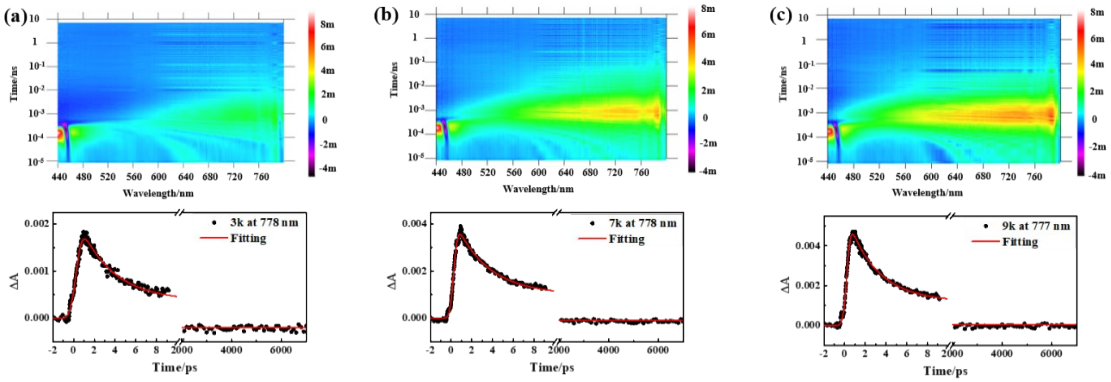

Figure S15. (a-c) Bird's eye plots of femtosecond transient absorption spectra of the Sb nanosheets in NMP solvent pumped at 400 nm (400 nJ). Representative corresponding decay curves recorded at ~770nm of femtosecond transient absorption spectra are exhibited below, respectively. Sb nanosheets were prepared through different centrifugated speed. The RCF are (a) 600 g, (b) 3400 g and (c) 5600 g, respectively.

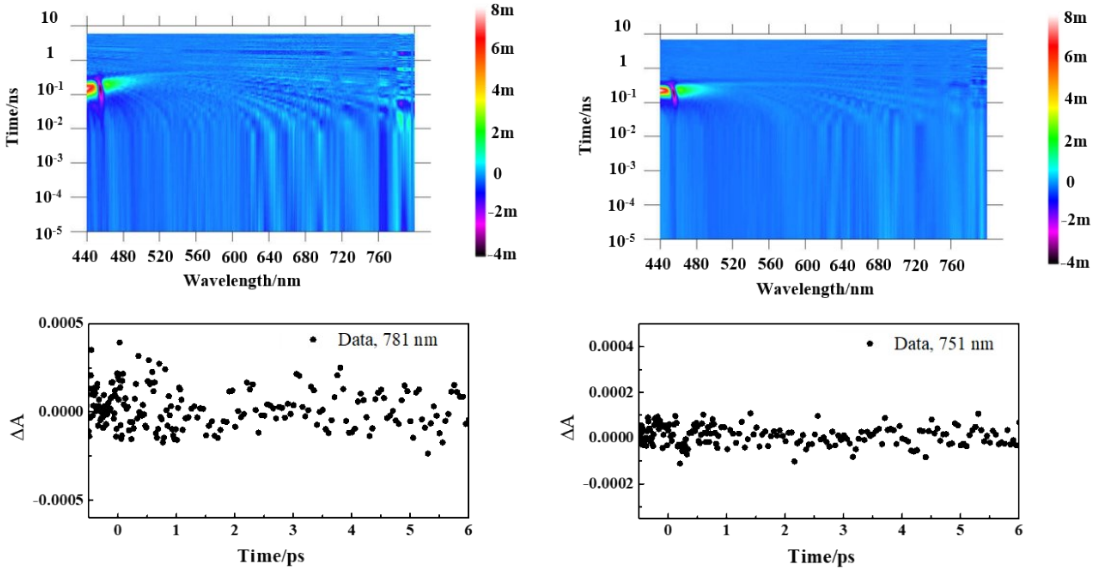

Figure S16. Bird's eye plots of femtosecond transient absorption spectra of the Sb_2O_3 dispersed in NMP solvent pumped at 400 nm (left: 400 nJ, right: 1.20 μJ). Representative corresponding decay curves of femtosecond transient absorption spectra are exhibited below, respectively.

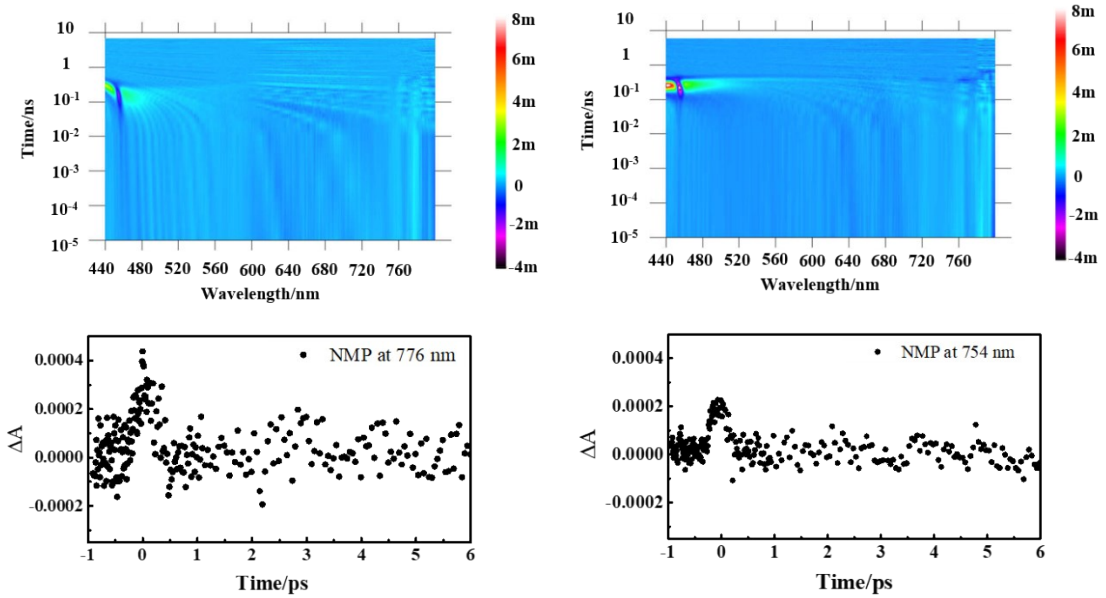

Figure S17. Bird's eye plots of femtosecond transient absorption spectra of NMP solvent pumped at 400 nm (left: 400 nJ, right: 1.20 μJ). Representative corresponding decay curves of femtosecond transient absorption spectra are exhibited below, respectively.

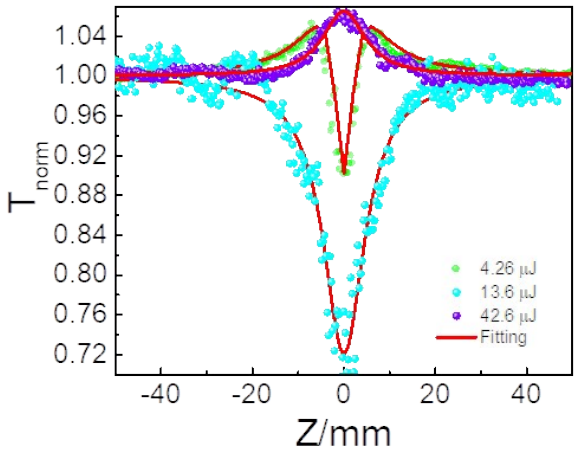

Figure S18. Z-scan open aperture and fitted curves (solid curves) of the 10000 g Sb nanosheets film. The linear transmittance was adjusted to 0.76 at the excitation of 532 nm.

Different decay curves of gradient centrifugated samples at a higher exciton pump laser energy (2.4 μJ) is collected as well (**Figure S19**). The changes in absorption show different. The ΔA is negative in low rotation speed prepared sample, indicating a ground state bleaching behavior, which induced SA property. In contrast, the signals became positive in high rotation speed prepared samples, which is ESA

behavior, leading to an RSA behavior.

At low pump power (400 nJ), all of the samples displayed a positive signal at the beginning and then decreases to negative signals eventually. The negative value indicates the ground state bleaching (GSB) signal is dominant in the competition of excited state absorption (ESA). The GSB behavior may induce SA as we demonstrated.[15] With the improvement of pump energy (2.4 μJ), 10000 g sample presents nearly no negative signals compared to others, revealing that ESA is dominant. The ESA is considered to be the reason inducing RSA behavior.[16]

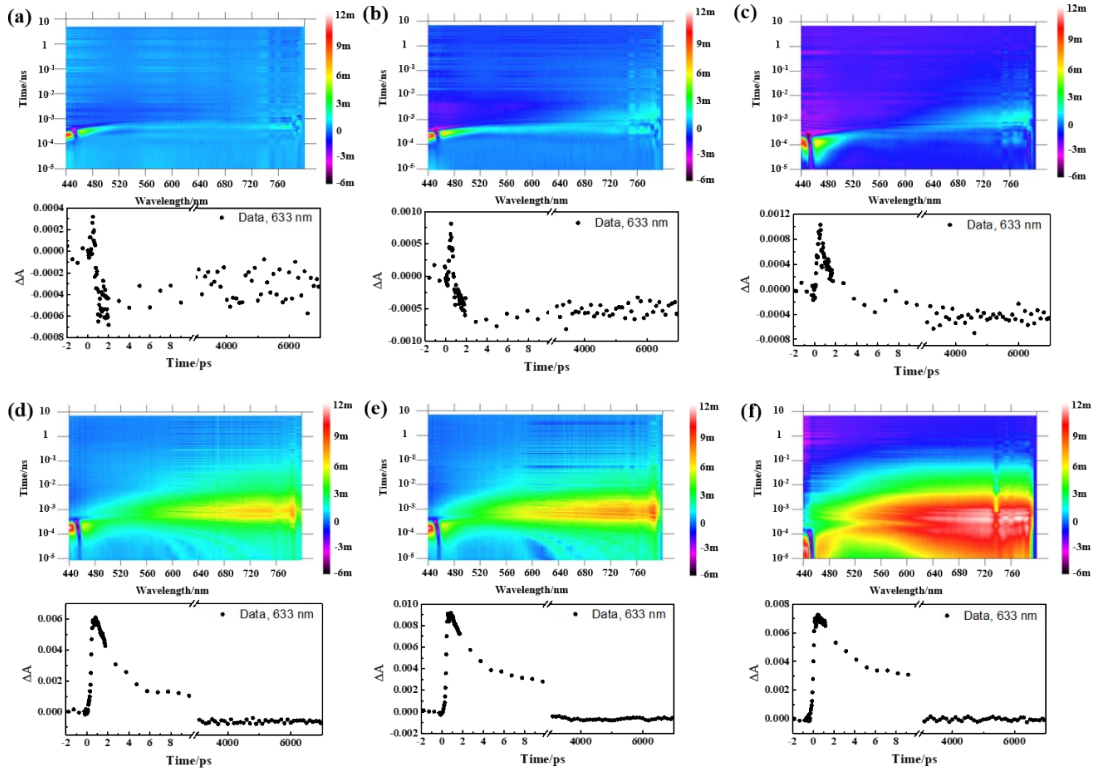

Figure S19. (a-f) Bird's eye plots of femtosecond transient absorption spectra of the Sb nanosheets in NMP solvent pumped at 400 nm (2.4 μJ). Representative corresponding decay curves recorded at 633nm of femtosecond transient absorption spectra are exhibited below, respectively. Sb nanosheets were prepared through different centrifugated speed. Centrifuging speeds are (a) 70 g (1k), (b) 630 g (3k), (c) 1700 g (5k), (d) 3400 g (7k), (e) 5600 g (9k), and (f) 10000 g (12k) samples, respectively.

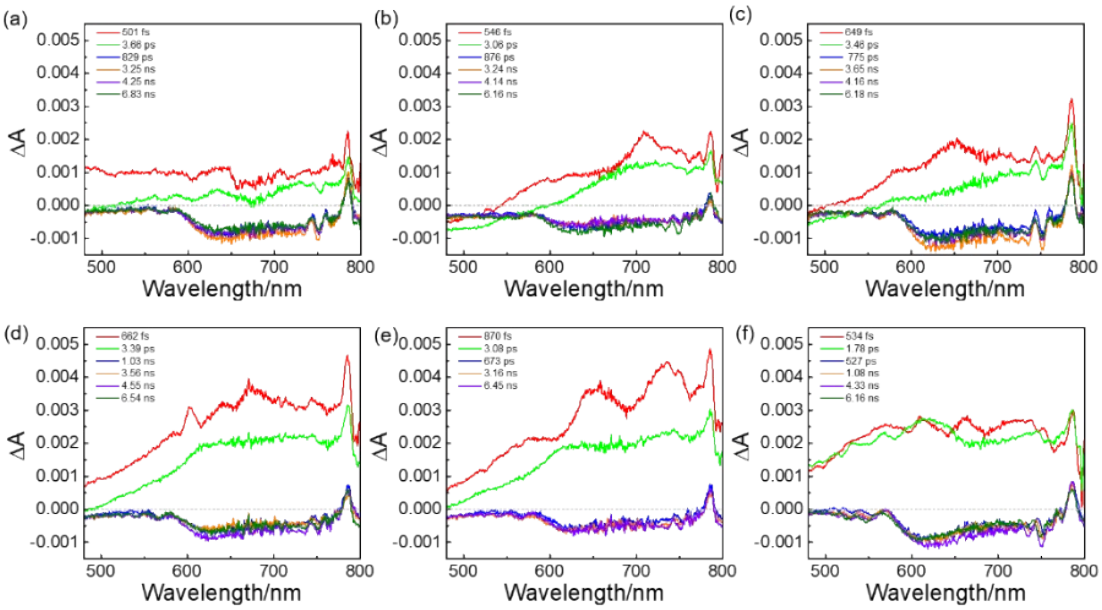

Figure S20. Selected representative fs-TAS spectra of the Sb nanosheet dispersion prepared through (a) 70 g (1k), (b) 630 g (3k), (c) 1700 g (5k), (d) 3400 g (7k), (e) 5600 g (9k), and (f) 10000 g (12k) samples, respectively. The pump power is 400 nJ.

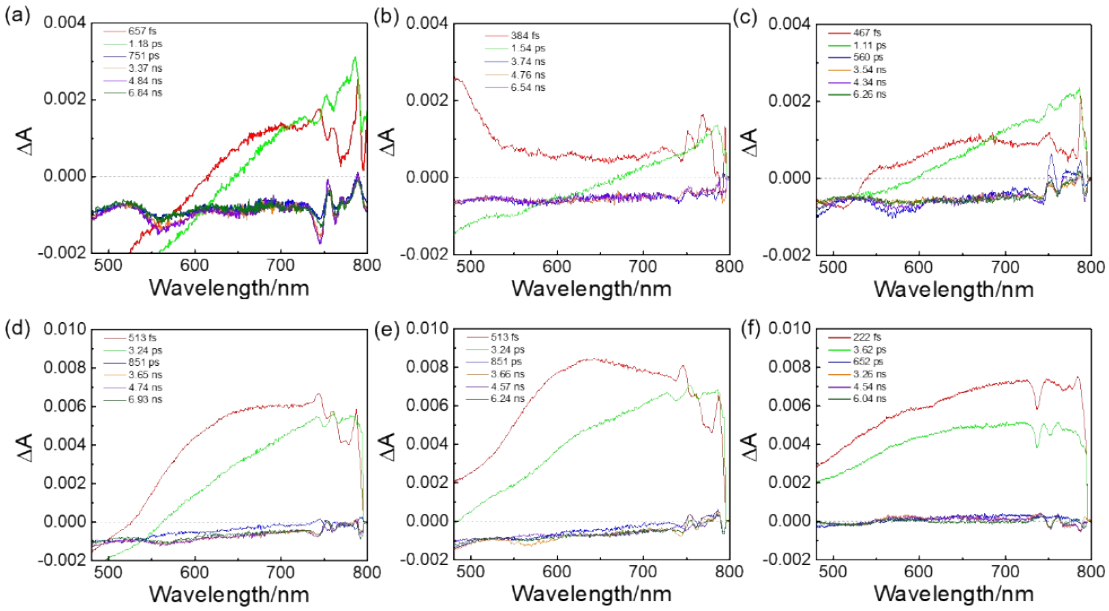

Figure S21. Selected representative fs-TAS spectra of the Sb nanosheet dispersion prepared through (a) 70 g (1k), (b) 630 g (3k), (c) 1700 g (5k), (d) 3400 g (7k), (e) 5600 g (9k), and (f) 10000 g (12k) samples, respectively. The pump power is 2.4 μJ.

Reference:

1. J. Q. Wang, D. M. Feng, W. H. Wu, M. X. Zeng and Y. Li, *Polym Degrad Stabil*, 1991, **31**, 129-140.
2. M. P. Seah and W. A. Dench, *Surface and Interface Analysis*, 1979, **1**, 2-11.
3. B. D. Ratner and D. G. Castner, *Surface Analysis – The Principal Techniques*, 2009.
4. C. Gibaja, M. Assebban, I. Torres, M. Fickert, R. Sanchis-Gual, I. Brotons, W. S. Paz, J. J. Palacios, E. G. Michel, G. Abellan and F. Zamora, *Journal of Materials Chemistry A*, 2019, **7**, 22475-22486.
5. J. N. Gu, Z. G. Du, C. Zhang, J. G. Ma, B. Li and S. B. Yang, *Adv. Energy Mater.*, 2017, **7**, 1700447.
6. C. Gibaja, D. Rodriguez-San-Miguel, P. Ares, J. Gomez-Herrero, M. Varela, R. Gillen, J. Maultzsch, F. Hauke, A. Hirsch, G. Abellan and F. Zamora, *Angew. Chem., Int. Ed.*, 2016, **55**, 14345-14349.
7. X. Wang, J. He, B. Zhou, Y. Zhang, J. Wu, R. Hu, L. Liu, J. Song and J. Qu, *Angew. Chem., Int. Ed.*, 2018, **57**, 8668-8673.
8. W. Z. Lin, Y. P. Lian, G. Zeng, Y. Y. Chen, Z. H. Wen and H. H. Yang, *Nano Research*, 2018, **11**, 5968-5977.
9. J. N. Coleman, M. Lotya, A. O'Neill, S. D. Bergin, P. J. King, U. Khan, K. Young, A. Gaucher, S. De, R. J. Smith, I. V. Shvets, S. K. Arora, G. Stanton, H. Y. Kim, K. Lee, G. T. Kim, G. S. Duesberg, T. Hallam, J. J. Boland, J. J. Wang, J. F. Donegan, J. C. Grunlan, G. Moriarty, A. Shmeliov, R. J. Nicholls, J. M. Perkins, E. M. Grieveson, K. Theuwissen, D. W. McComb, P. D. Nellist and V. Nicolosi, *Science*, 2011, **331**, 568-571.
10. K. Varoon, X. Zhang, B. Elyassi, D. D. Brewer, M. Gettel, S. Kumar, J. A. Lee, S. Maheshwari, A. Mittal, C. Y. Sung, M. Cococcioni, L. F. Francis, A. V. McCormick, K. A. Mkhoyan and M. Tsapatsis, *Science*, 2011, **334**, 72-75.
11. F. Behnoudnia and H. Dehghani, *RSC Adv.*, 2014, **4**, 39672-39677.
12. M. Inam, R. Khan, D. Park, Y.-W. Lee and I. Yeom, *Water*, 2018, **10**.
13. C. M. Hansen, *Hansen Solubility Parameters: A User's Handbook*, 2007.

14. L. F. Gao, J. Y. Xu, Z. Y. Zhu, C. X. Hu, L. Zhang, Q. Wang and H. L. Zhang, *Nanoscale*, 2016, **8**, 15132-15136.
15. Q. Q. Yang, R. T. Liu, C. Huang, Y. F. Huang, L. F. Gao, B. Sun, Z. P. Huang, L. Zhang, C. X. Hu, Z. Q. Zhang, C. L. Sun, Q. Wang, Y. L. Tang and H. L. Zhang, *Nanoscale*, 2018, **10**, 21106-21115.
16. K. G. Zhou, M. Zhao, M. J. Chang, Q. Wang, X. Z. Wu, Y. Song and H. L. Zhang, *Small*, 2015, **11**, 694-701.